

Using Fast Sequential Asymmetric Fanbeam Transmission CT for Attenuation Correction of Cardiac SPECT Imaging

Edward F. Hollinger, Srecko Loncaric, Dan-Chu Yu, Amjad Ali and Wei Chang

Department of Diagnostic Radiology and Nuclear Medicine and Section of Medical Physics, Rush-Presbyterian-St. Luke's Medical Center, Chicago, Illinois

The objective of this study was to determine the feasibility of using a fast (short-duration) transmission computed tomogram (TCT), acquired immediately before or after the emission CT, to correct for photon attenuation in cardiac SPECT. **Methods:** The asymmetric fanbeam geometry with a ^{99m}Tc line source was used to acquire TCTs after conventional cardiac emission CT imaging on a triple-head SPECT system. The TCTs were reconstructed to generate patient-specific attenuation maps, which were used with an iterative maximum likelihood algorithm to reconstruct attenuation-corrected cardiac SPECT studies. The results of attenuation correction based on TCTs as short as 1 min were compared with long-duration transmission imaging for a phantom and several human studies. **Results:** Attenuation correction based on asymmetric fanbeam TCT significantly improves the uniformity of images of a uniform tracer distribution in a cardiac-thorax phantom configured to simulate a large patient. By using a high-activity line source and a rapid camera rotation, a suitable attenuation map for this phantom can be obtained from a 4-min TCT. A similar result is obtained for patients with thorax widths of <40 cm. **Conclusion:** A sequential imaging protocol for acquiring a fast TCT can be used for attenuation correction of cardiac SPECT imaging. The sequential TCT can be acquired without significantly extending the duration of the imaging study. This method provides a way to perform attenuation correction on existing triple-head SPECT systems without extensively modifying the system.

Key Words: attenuation correction; transmission CT; SPECT

J Nucl Med 1998; 39:1335-1344

A significant limitation on the accuracy of cardiac SPECT is the attenuation of emission photons in the thorax. Attenuation induces artifacts that can simulate or obscure clinically significant perfusion abnormalities (1-4). Therefore, several approaches for performing attenuation correction (AC) have been examined as methods for improving the accuracy of clinical cardiac SPECT.

The problem of correcting for photon attenuation in the thorax is complicated by the markedly different attenuation coefficients of tissues such as lung, bone and adipose tissue. The amount of attenuation is also dependent on patient size, habitus and position during imaging. Therefore, AC techniques that assume uniform distributions of attenuating media (5) are not suitable for cardiac imaging. Further, simply altering the SPECT acquisition protocol, i.e., changing the patient position or the extent of the gantry rotation, often cannot eliminate the effects of attenuation (6,7). Instead, most techniques currently under investigation use direct measurements of the distribution of attenuating media in the thorax, usually obtained by perform-

ing transmission measurements using an external radioactive source (4,8-20).

Two major approaches to acquiring these transmission CTs (TCTs) have been described. With simultaneous imaging protocols (4,8-12), the TCT and emission CT (ECT) scans are acquired concurrently. With sequential protocols (13-20), the TCT is acquired immediately before or after acquisition of the ECT. Each approach has inherent advantages and disadvantages. Simultaneous imaging reduces the problem of matching the patient position between TCT and ECT, but results in crosstalk between the emission and transmission sources. This necessitates a crosstalk correction before image reconstruction. Using a sequential protocol significantly reduces the problem of crosstalk but may prolong total imaging duration and provide additional opportunity for patient motion.

Compared to other radioactive source configurations, e.g., sheet sources, uniform-activity line sources are relatively easy to produce. Therefore, many AC techniques make use of a scanning line source and parallel collimation or a fixed line source and fanbeam collimation for acquiring the TCT. Scanning line source techniques generally require a simultaneous imaging protocol because of the time required to scan the source across each projection view. Fanbeam techniques have been applied with both sequential and simultaneous protocols (9,16). The primary advantage of the scanning line source and parallel collimation is that the transmission field of view (FOV) can be as large as the useful FOV of the gamma camera. However, the moving line source adds complexity to the SPECT system, and for most triple-head SPECT systems it is difficult to design a scanning line source that will not interfere with one or both of the cameras not used for transmission imaging. Although implementing a fixed line source and fanbeam collimation is generally simpler than implementing a scanning line source, fanbeam TCT often suffers from a limited transmission FOV. This is particularly true for many triple-head SPECT systems because the design of the gantry limits the focal length of the fanbeam. The result of a limited FOV is truncation of the transmission projections, which can compromise the quality of the attenuation maps. Several studies have investigated techniques for augmenting the truncated TCT, e.g., using information from scattered photons, to derive the complete attenuation map (21,22). Others have proposed replacing transmission imaging with segmentation and tissue boundaries determined from emission imaging (23). In this study, we enlarged the FOV by using an asymmetric fanbeam (AsF) geometry (17-19) for the TCT. The AsF geometry is similar to other fanbeam geometries in that it uses a radioactive line source at the focus of a fanbeam collimator. However, this implementation of the AsF geometry allows a TCT with an FOV (39 cm) that is nearly as large as the FOV provided by the

Received Apr. 8, 1997; revision accepted Oct. 13, 1997.

For correspondence or reprints contact: Edward F. Hollinger, MS, Section of Medical Physics, Rush-Presbyterian-St. Luke's Medical Center, 1653 West Congress Pkwy., Chicago, IL 60612.

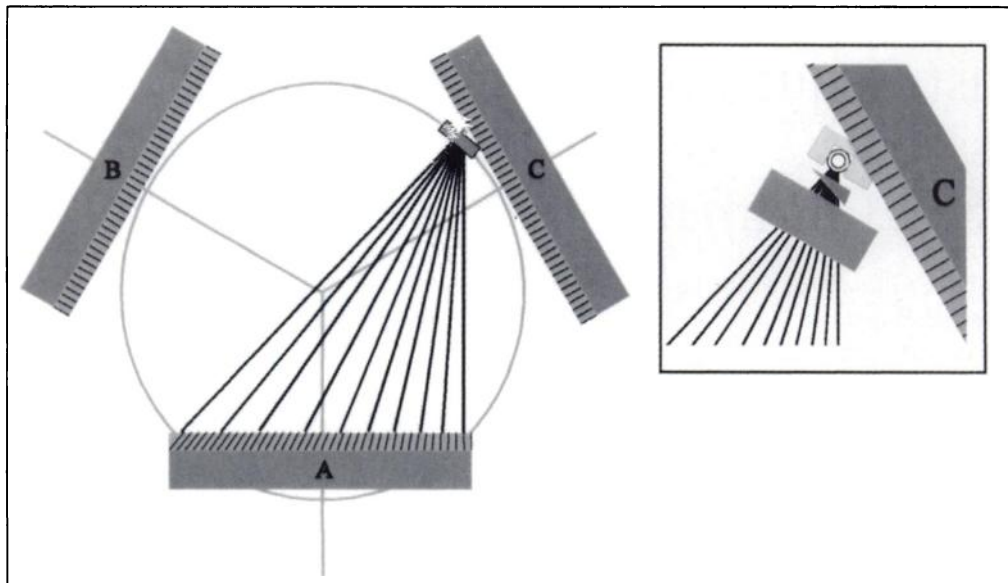


FIGURE 1. Schematic diagram of AsF-TCT acquisition system on triple-head gamma camera. Camera A has AsF collimator. Slightly more than half of FOV for TCT is obtained with camera as shown; the other half of FOV is obtained when camera A has rotated 180°. Camera C holds mounting hardware for line source assembly. (Inset) Enlarged view of line source assembly, including wedge filter and transverse slat source collimator.

camera (40 cm). A schematic of the AsF geometry is shown in Figure 1.

Previously, we presented results illustrating the quality of long-duration (10–20-min) AsF-TCT images of phantoms and a human subject (19). However, simulation studies have indicated that the quality of AC cardiac SPECT is dominated by the statistical quality of the ECT even for relatively short TCT durations (24). Furthermore, even short-duration TCTs contain significant anatomic information (25). Therefore, in this study, we focused on determining whether fast, sequential AsF transmission scans can provide an attenuation map of sufficient quality for AC of cardiac SPECT. By using a high-activity line source, we can reduce the time required for acquiring the TCT to a fraction of that required for the ECT acquisition. Thus, the overall imaging duration is not extended significantly, whereas problems associated with photon crosstalk are essentially eliminated. We evaluated this method by using an anthropomorphic thorax phantom with a cardiac insert simulating normal ^{201}Tl uptake in the heart and attenuation maps derived from TCTs with durations from 1 to 20 min. Finally, the results of AC based on short- and long-duration TCTs for several clinical ^{201}Tl SPECT studies were compared.

MATERIALS AND METHODS

System Overview

Four primary components were added to a conventional triple-head SPECT system to acquire the AsF-TCT: a transmission line source (8,10,16,26), a wedge filter to modulate the source flux (8,16,19), a transverse slat source collimator and an AsF collimator. We upgraded and optimized these components based on the results of our previous studies (19). A schematic diagram of the AsF hardware installed on a triple-head SPECT system is shown in Figure 1.

Transmission Source Assembly

The line source consists of a 30-cm-long, 2.8-mm inner diameter plastic tube within a Lucite enclosure. The source was filled with 2220–2590 MBq (60–70 mCi) of an aqueous solution of $^{99\text{m}}\text{Tc}$ -chloride. The center 26 cm of the line source was opposite the active region of the AsF collimator. A lead wedge filter was mounted adjacent to the line source, as shown in Figure 1 (inset). The wedge filter is composed of multiple layers of 0.18-mm-thick

lead foil arranged in a stairstep pattern. It is oriented so that rays passing from the line source through the wedge filter strike the filter at oblique angles relative to the steps. The wedge filter is used to modify the spatial distribution of flux from the line source to optimize the TCT acquisition.

Source Collimator

A 7.5-cm (wide) \times 4-cm (high) transverse slat collimator was mounted immediately adjacent to the wedge filter. It is composed of 0.4-mm-thick lead foils separated by 4-mm Styrofoam spacers. The source collimator removes photons that are emitted from the source in directions other than perpendicular to the line source, e.g., cross-plane photons. Eliminating these photons reduces the dose the patient receives from the TCT and reduces the effects of scatter in the TCT.

Asymmetric Fanbeam Collimator

The camera opposite the line source was fitted with a low-energy, high-resolution AsF collimator (Nuclear Fields, St. Marys, New South Wales, Australia). This collimator has hexagonal cast holes and lead septa that form a two-dimensional asymmetric fan with a 52-cm focal length. This AsF collimator has a sensitivity of 87 cts/MBq/sec (3.2 cts/ μCi /sec) and a geometric resolution of 7.5 mm at 10 cm from the front surface of the collimator (based on the National Electrical Manufacturers Association standards).

Phantom Studies

We extended our previous AsF studies by using attenuation maps derived from 1- to 20-min duration TCTs for AC of cardiac SPECT. To evaluate the feasibility of this approach, we used an anthropomorphic thorax phantom (Data Spectrum Corp., Hillsborough, NC). This phantom consists of an elliptical cylinder (32-cm lateral diameter \times 23-cm anterior–posterior diameter) containing inserts representing the lungs, vertebral column and heart. Three 2.5-cm (axial length) Lucite rings were fitted on the outside of the cylinder to simulate the presence of additional anterior and lateral chest-wall adipose tissue and breasts. The dimensions of the thorax phantom with these rings in place is 38.5 cm (lateral) \times 26 cm (anterior–posterior). The vertebral column is simulated by a 3.8-cm-diameter Teflon cylinder that extends along the length of the phantom. The lungs contain Styrofoam beads, representing nearly air-equivalent material. For these studies, water was not added to

the lung inserts to maximize the inhomogeneity of attenuators, making the effects of attenuation more nonuniform.

The cardiac insert consists of two concentric semielliptical chambers oriented along an axis similar to the anatomic orientation of the heart in the thorax. The outer chamber (6.1-cm diameter \times 9.3-cm length) represents the myocardium. The inner chamber (4.1-cm diameter \times 8.3-cm length) represents the myocardial blood pool. Myocardial uptake of ^{201}Tl was simulated by uniformly distributing 84 kBq/ml (2.3 $\mu\text{Ci/ml}$) ^{201}Tl in the outer cylinder of the insert; the inner chamber was filled with water. To simplify the imaging situation, no radioactivity was placed in the lungs or thorax of the phantom.

Human Studies

A total of 15 individuals, including volunteers and patients scheduled to undergo ^{201}Tl exercise treadmill testing, participated in a feasibility study of AsF attenuation correction. The results of two representative studies, each of which involved multiple TCTs, are shown. Transmission CTs were acquired immediately after the conventional clinical stress and rest SPECT imaging protocols. The protocol for AsF imaging was approved by the human investigations committee of the medical center, and all subjects gave informed consent before beginning the study.

Acquisition Protocol

All studies were conducted using a triple-head gamma camera (GMS 9300A; Toshiba America Medical Systems, Tustin, CA). For patient studies, stress and rest ^{201}Tl ECTs were acquired using our routine clinical protocol except that a circular rather than an elliptical orbit was used. The ECT was acquired into a 64×64 pixel matrix with a 120° step-and-shoot gantry rotation and a 4° step size for a total of 360° of ECT data. Each projection was acquired for 30 sec. A 30% window on the 67-keV photopeak and a 20% window centered on the 167-keV photopeak of ^{201}Tl were used.

After completion of our standard clinical ECT protocol, the position of the bed was marked, the patient was instructed not to move and the bed was retracted from the camera aperture. The prefilled $^{99\text{m}}\text{Tc}$ line source assembly was mounted, and the AsF collimator was placed on the opposite scintillation camera. The bed was returned to the initial position, and the TCT was acquired using a continuous 360° rotation and 180 projection views. A 2° step size was used to minimize rebinning artifacts during filtered back-projection reconstruction of the TCT. Data were acquired into a 64×64 matrix with a 20% energy window centered on the 140-keV photopeak of $^{99\text{m}}\text{Tc}$. The total duration of the TCT acquisitions ranged from 1 to 20 min for the phantom measurements. For volunteers and patients, at least one short (1- to 4-min) and one long (10-min) TCT were acquired for each SPECT study.

After each set of transmission measurements, we acquired a 1.5×10^6 count planar blank scan, with the TCT configuration but without a patient. The blank scan is used during the reconstruction of the TCT to correct for variations in the transmission source activity and inhomogeneities in the transmission photon flux (8,16,19,26). Typically, the blank scan was acquired after a delay that allowed the $^{99\text{m}}\text{Tc}$ line source to decay to an activity where the counting rate achieved during the blank scan was close to that obtained during clinical imaging.

Image Reconstruction

Details of filtered backprojection reconstruction of the AsF-TCT have been provided previously (27). Briefly, the first step in reconstructing the TCT is to scale the number of counts in the blank scan to that of the measured transmission data. This is accomplished by comparing the number of counts in a region of interest (ROI) on a portion of the TCT where photons do not pass

through the patient to an equivalent ROI on the blank scan. Next, projections representing line integrals of linear attenuation are generated by taking the natural logarithm of the ratio of the scaled blank scan to the measured transmission projections. Then, each projection view is extended by combining the originally sampled region with information from several opposing projections. The extended projections are filtered using a Butterworth filter with order $n = 8$ and cutoff frequency $f_c = 0.2$ of the Nyquist frequency. Finally, the portion of each extended projection on the original side of the axis of rotation (i.e., the unextended data) is backprojected using a ramp filter to complete the TCT reconstruction.

The attenuation map is obtained from transaxial slices of the reconstructed TCT. Because the ECT and TCT measurements use sources with different photon energies, the attenuation map must be scaled to take into account the energy dependence of the attenuation coefficients. This is accomplished by multiplying the attenuation map by a constant scaling factor (14). The scaling factor was initially determined by comparing the tabulated broadbeam attenuation coefficients for $^{99\text{m}}\text{Tc}$ and ^{201}Tl (28). This scaling factor was further refined empirically by adjusting the attenuation coefficient to maximize the uniformity of attenuation-corrected images of a uniform ^{201}Tl distribution inside a water phantom. Based on this process, we use a scaling factor of 1.06, which yields an attenuation coefficient of $\mu_t = 0.16 \text{ cm}^{-1}$ for tissue, somewhat lower than the reported value of $\mu_t = 0.183 \text{ cm}^{-1}$. These results were confirmed by examining the uniformity of phantom and patient images with maps adjusted by several scaling factors.

The emission studies are prefiltered using a Butterworth filter with order $n = 8$ and cutoff frequency $f_c = 0.2$ of the Nyquist frequency. They are reconstructed using an iterative maximum likelihood-expectation maximum (ML-EM) algorithm incorporating the TCT-derived attenuation maps (29). Thirty iterations of the ML-EM algorithm are used.

RESULTS

Phantom Studies

Figure 2 shows the results of 1- to 20-min TCTs of the thorax phantom. These studies were acquired with the same myocardial ^{201}Tl activity as that used for the ECT acquisition. During acquisition, the counting rate (CR) of the camera acquiring the TCT is typically about 40 kcps. This CR results in $\sim 1 \times 10^5$ counts in each TCT slice per minute of TCT acquisition. The images and linear profiles are of the same 1-pixel-thick slice of the midventricular region of the phantom. The images and corresponding profiles are all of sufficient quality to distinguish the air-filled lung regions, the vertebral column and the Lucite rings. The short-duration studies (1- and 2-min) show some noise-induced artifacts. Of these, the most significant is the apparent "hole" located in the center of the phantom. The hole is largest in the 1-min TCT and smaller, but still present, in the 2-min TCT; it is the result of the center of the phantom being imaged by photons near the most sharply angled edge of the AsF geometry (e.g., the rays entering the left side of camera A in Figure 1). These transmission photons encounter the longest path through the patient for all of the projection views. For short-duration TCTs, the high attenuation encountered by these photons results in some pixels with zero counts in the corresponding projection views. This artifact is not observed when the TCT duration is 4 min or longer. The local overshoots near interfaces between dissimilar media result from the use of a high-resolution convolution filter in the reconstruction. These overshoots could be removed, at the expense of resolution, by

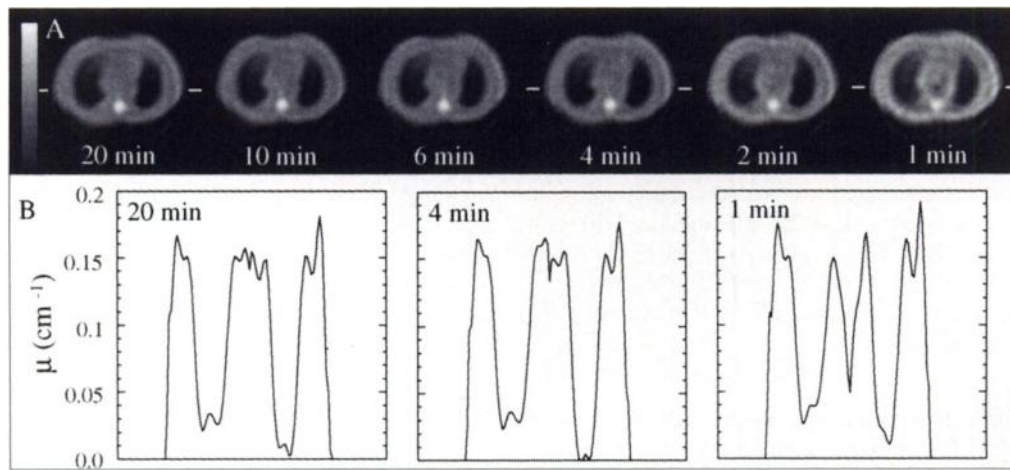


FIGURE 2. Results of 1- to 20-min duration AsF-TCT imaging of anthropomorphic thorax phantom. (A) Single-pixel-thick midventricular slices. (B) Plots represent pixel values for horizontal profile at level indicated by hash marks; total width of each plot is 128 pixels. Most significant artifact in short-duration scans is hole in center of phantom that is visible in 1-min TCT and marginally observable in 2-min TCT.

smoothing the images. However, the AC algorithm is not very sensitive to these local effects because calculating the line integrals along the emission photon paths effectively provides additional smoothing of the attenuation map.

The results of uncorrected (NC) and AC ^{201}Tl SPECT studies for the thorax phantom are shown in Figures 3 and 4. The ECT duration was 20 min, and all studies were reconstructed using the ML-EM algorithm. NC studies reconstructed with the ML-EM algorithm show no significant differences from the same data reconstructed with filtered backprojection. For each subject, the reconstructed SPECT images were reoriented to horizontal long axis (HLA), vertical long axis (VLA) and short-axis (SA) views using the same parameters for both the NC and AC studies. For phantom studies, the SA slice of the NC study showing the most overall nonuniformity was subjectively determined by examining SA and VLA slices as well as summed circumferential profiles. The SA slice selected was assumed to demonstrate the most severe attenuation artifact and was used for subsequent analysis of all NC and AC results for that study. Next, polar plots were calculated using all of the SA views for the study and a method similar to that described by Garcia et al. (30). Finally, a local and a global summed circumferential profile were calculated for each NC or AC reconstruction. The local summed circumferential profiles were determined by summing pixel values as a function of angle for an annular ROI set on the most attenuated SA slice determined previously. The inner and outer radii of the ROI were set at the inner and outer edges of the myocardial activity distribution. The global profile represents the results of a similar calculation for the polar plot of the entire myocardium, with the limits of the ROI set at the inner and outer edges of the polar plot. The same local and global ROIs were used for the NC and all of the AC studies for each subject.

The top panel of Figure 3 shows the results of NC cardiac SPECT for a uniform ^{201}Tl tracer distribution located inside the thorax phantom. The prominent attenuation artifact observed, especially in the inferior and inferior-septal regions, is greater than that typically observed in patient studies for several reasons. First, the axial length of the lungs is smaller for the phantom than for most patients. This results in a high diaphragm region with large attenuation. Second, the lungs were filled with air rather than simulating typical lung tissue, which is $\sim 30\%$ the density of water. This results in a greater difference in attenuation between photons passing through the lung regions and

photons passing through the remainder of the phantom. These exaggerated (from typical anatomy) imaging conditions were used to provide a worst-case scenario in which attenuation effects would be more severe than those generally encountered in routine clinical imaging.

The remainder of Figure 3 shows the results of AC for phantom studies based on attenuation maps derived from TCTs with 1- to 20-min durations. The AC study based on a 20-min TCT shows a 35% increase in counts in the inferior wall relative to those in the NC study. Although the uniformity of the myocardium is significantly improved when AC is applied, some local nonuniformities remain. The likely cause of these nonuniformities is that the same phantom configuration that maximizes inhomogeneities in attenuation results in inhomogeneous scatter of emission photons. The nonuniformities are significantly more severe than those observed for patient studies, probably because the use of air-equivalent lungs in the phantom results in larger and sharper variations in photon-absorbing material than those found in humans. Furthermore, the apparent increase in activity in the anterior wall may be partially attributable to the lack of compensation for distance-dependent collimator resolution (8).

To determine the shortest TCT that can be used for AC, we compared AC based on short-duration TCTs with the NC and long-duration TCT with the AC studies. Reducing the TCT duration to 4 min had little effect on the results of AC. Further reducing the TCT duration to 2 min resulted in a mild undercorrection, with inferior wall counts increased by 30% relative to those in the NC study (5% less than AC from the 20-min TCT study). This undercorrection is probably caused by the appearance of a mild form of the previously demonstrated hole near the center of the TCT image. When the TCT duration is reduced to 1 min, this artifact becomes more prominent. Attenuation correction based on the 1-min TCT shows a 20% increase in counts in the inferior wall relative to those in the NC study.

The impact of TCT duration on AC is demonstrated graphically in Figure 4. This figure shows single-slice and global anterior-inferior (A-I) wall ratios for the NC study (zero duration TCT) and studies corrected using TCTs with durations from 1 to 20 min. The A-I ratios were calculated with the same ROIs as those defined for the circumferential profiles, but using one annular 45° subregion centered at the 12 o'clock position (anterior wall) and one at the 6 o'clock position (inferior wall).

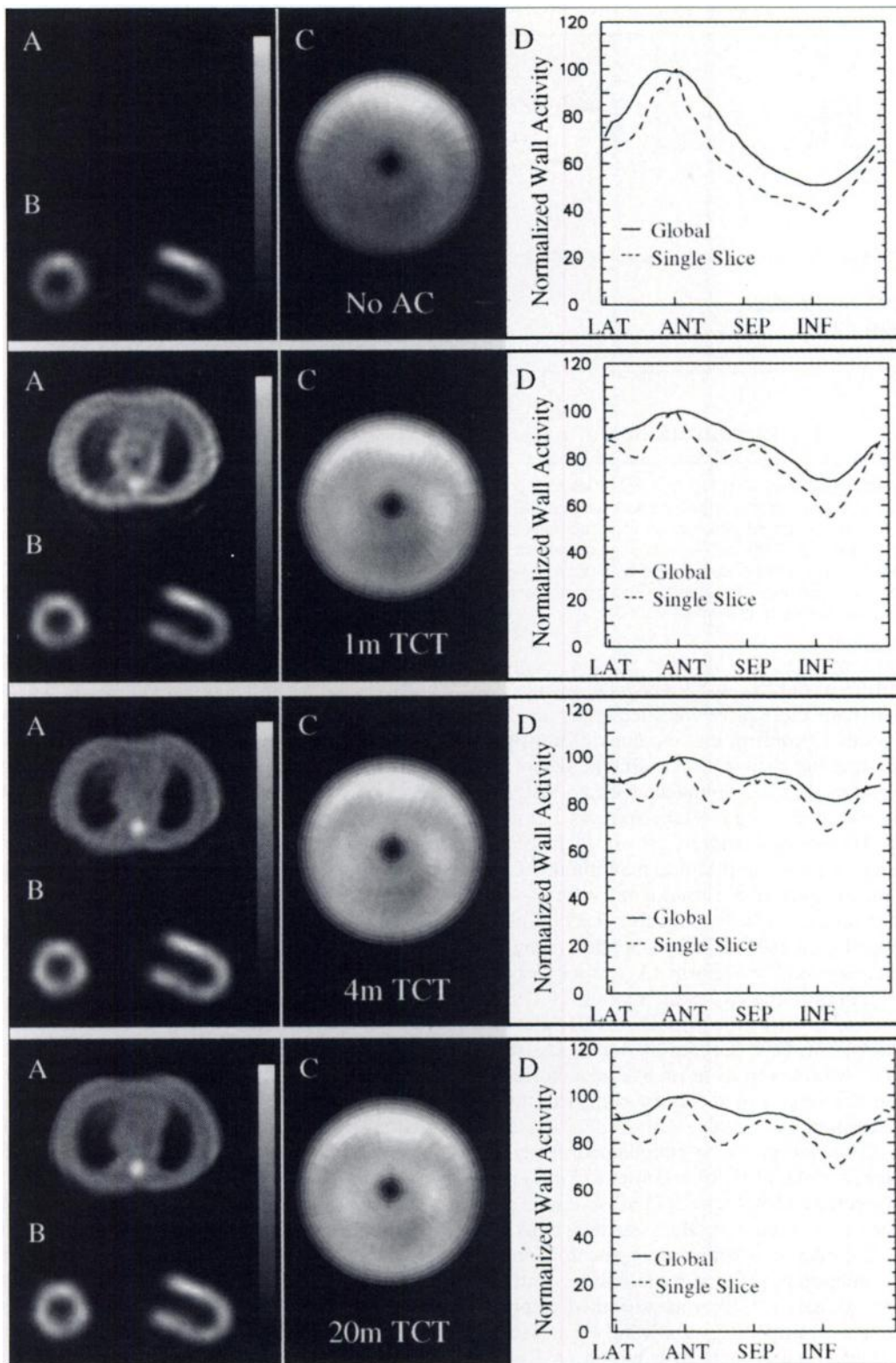


FIGURE 3. Results of NC and AC cardiac SPECT studies of cardiac insert located inside thorax phantom. Cardiac insert simulates uniform distribution of ^{201}Tl in myocardium. AC was based on maps derived from TCTs with 1-, 4- and 20-min durations. (A) Single-pixel-thick slice of TCT. Note that no TCT is acquired for NC study. (B) Short-axis and vertical long axis slices through region of heart demonstrate the most nonuniformity in NC study. (C) Polar map of simulated myocardium. (D) Summed circumferential profiles for SA slice shown in B and for myocardium as a whole (global profile).

The A-I ratio reflects the ratio of the total number of counts in these subregions. For the phantom configuration that simulates a large patient with significant attenuation, the A-I ratio shows marked improvement for AC based on a 1-min TCT relative to that in the NC study. A further significant improvement is observed when a 2-min TCT is used, and a slight improvement in uniformity is gained when the TCT duration is increased to

4 min. Increasing the TCT duration beyond 4 min has little effect on the A-I ratio.

Human Studies

For the human studies, a similar analysis was conducted. The SA slice with the most severe attenuation was initially subjectively chosen by examining SA and VLA slices and summed

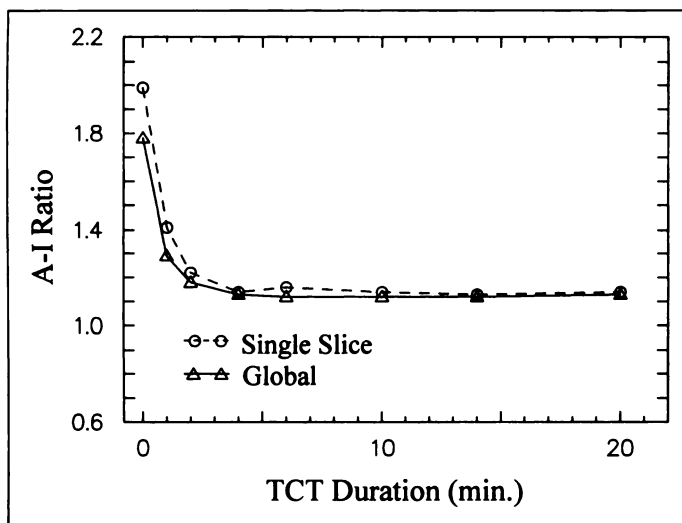


FIGURE 4. A-I wall ratios generated from NC and AC studies of uniform distribution of ^{201}Tl in cardiac insert imaged inside thorax phantom. NC study is represented by TCT duration of zero. Attenuation correction was calculated from TCTs with durations of 1–20 min; A-I ratio was calculated using 45° annular ROIs in anterior and inferior walls. Single-slice points represent A-I ratios for most nonuniform SA slice of NC study. Global points represent effects of attenuation on myocardium as a whole.

circumferential profiles of the NC study. Then, the selected NC slice was compared with the equivalent slice from the long-duration TCT AC study to confirm that the nonuniformity was caused by attenuation rather than by a physiologic defect.

Patient 1 was a 44-yr-old male volunteer with no history of cardiac disease. He weighed 72 kg (160 lb) and was 172 cm (5 feet 8 inches) tall. Uncorrected and AC stress ^{201}Tl SPECT studies for this patient are shown in Figure 5. Without AC, the effects of attenuation are noted in the inferior and inferior-septal regions of the myocardium (A-I ratios: local = 1.29, global = 1.18). When AC based on a 10-min TCT is applied, images of the myocardium become nearly uniform (A-I ratios: local = 1.01, global = 0.97). Performing AC using a 2-min TCT yields essentially the same result (A-I ratios: local = 1.01, global = 0.96). Further reducing the TCT duration to 1 min (A-I ratio: local = 1.09, global = 1.02) results in an 8% undercorrection for the most attenuated region of the heart compared to AC based on the long-duration TCT study.

Patient 2 was a 37-yr-old man who complained of atypical chest pain. He weighed 75 kg (165 lb) and was 175 cm (5 feet 9 inches) tall. Uncorrected and AC rest ^{201}Tl SPECT studies for this patient are shown in Figure 6. Because this individual lacked other clinical evidence of impaired myocardial perfusion, the apparent reduction in activity in the inferior wall (A-I ratios: local = 1.46, global = 1.29) was attributed to photon attenuation. AC using a 10-min TCT significantly increases the uniformity of the myocardial activity distribution (A-I ratios: local = 1.10, global = 1.02). A similar result is obtained when a 4-min TCT is used (A-I ratios: local = 1.07, global = 0.99). When a 2-min TCT (not shown) is used, the study is slightly undercorrected (A-I ratios: local = 1.16, global = 1.07) relative to the long-duration TCT study. Thus, AC confirms the initial clinical suspicion that photon attenuation, rather than decreased perfusion, was responsible for most of the nonuniformity of the SPECT study.

DISCUSSION

Several studies have suggested that AC may increase the sensitivity and specificity of cardiac SPECT (4,31). However,

the issue of simultaneous versus sequential acquisition of the TCT and ECT studies remains controversial. To accurately characterize the efficacy of sequential techniques, as well as compare the merits of sequential and simultaneous techniques, it is necessary to determine the sequential TCT duration needed for accurate AC.

One significant concern about sequential AC protocols is that the time required to complete both the TCT and the ECT acquisitions will significantly extend the total duration of patient imaging. This raises concerns about increased likelihood of patient motion and the possibility of spatial misregistration between the ECT and TCT acquisitions. The results of this study indicate that, for the AsF geometry, extending the TCT acquisition beyond 4 min yields little improvement in AC even when significant attenuation artifact is seen, such as with the thorax phantom. For most cardiac patients, who have thorax widths of <40 cm, a 4-min TCT is sufficient for AC. The duration of the TCT could be further reduced by increasing the CR during the TCT. Many state-of-the-art camera systems have CR capabilities in excess of 220 kcps, more than twice that of the system used in this study. On such a system, it should be possible to obtain an adequate TCT in 2 min or less.

Although it is not as apparent, even simultaneous AC protocols require that total study duration be increased to obtain the same noise-equivalent images as an NC study. This results because some correction needs to be made for crosstalk, e.g., transmission source photons that are detected in the emission energy window(s). Several approaches have been proposed to address this problem (8,10,12,32). Some scanning line source AC techniques use a corresponding scanning window on the opposite camera where acquisition of the ECT is turned off while TCT data are acquired. Although this can reduce (but not eliminate) the amount of crosstalk, it also reduces the sensitivity of the SPECT system, requiring a longer acquisition to obtain the same number of counts in the ECT study. Other techniques use additional processing of the emission study to address the effects of transmission source crosstalk. However, this additional processing also adds noise to the ECT, requiring a longer acquisition to achieve the same noise-equivalent ECT data. Sequential techniques do not suffer from this form of crosstalk because the transmission source is removed or shielded while the ECT is acquired. Therefore, the duration of the ECT can be shorter than that for an equivalent simultaneous protocol yielding the same statistical and noise-equivalent SPECT data. Thus, it is likely that the total imaging duration is similar for simultaneous and sequential AC techniques.

A second possible form of crosstalk in both sequential and simultaneous protocols occurs when emission photons are detected in the TCT window. Using a high-resolution AsF collimator reduces the number of emission source photons in the transmission image because the imaging geometry is largely determined by the placement of the line source. Thus, most emission photons, but relatively few useful transmission photons, are removed by the collimator (33). For the current AsF system, the fraction of ^{201}Tl emission photons in the $^{99\text{m}}\text{Tc}$ transmission image was measured by performing a TCT acquisition on the thorax phantom with only the ^{201}Tl emission source present. To provide an estimate of the upper boundary for crosstalk, we used a relatively high ^{201}Tl background activity (compared to that typically encountered in clinical studies) of 70 kBq/ml (1.9 $\mu\text{Ci/ml}$) in the myocardium and 11 kBq/ml (0.30 $\mu\text{Ci/ml}$) in the remainder of the phantom except the lungs. The ratio of true transmission counts to crosstalk counts was calculated for each projection view. These results demonstrate that for ^{201}Tl , on the average, $0.34 \pm 0.12\%$ of

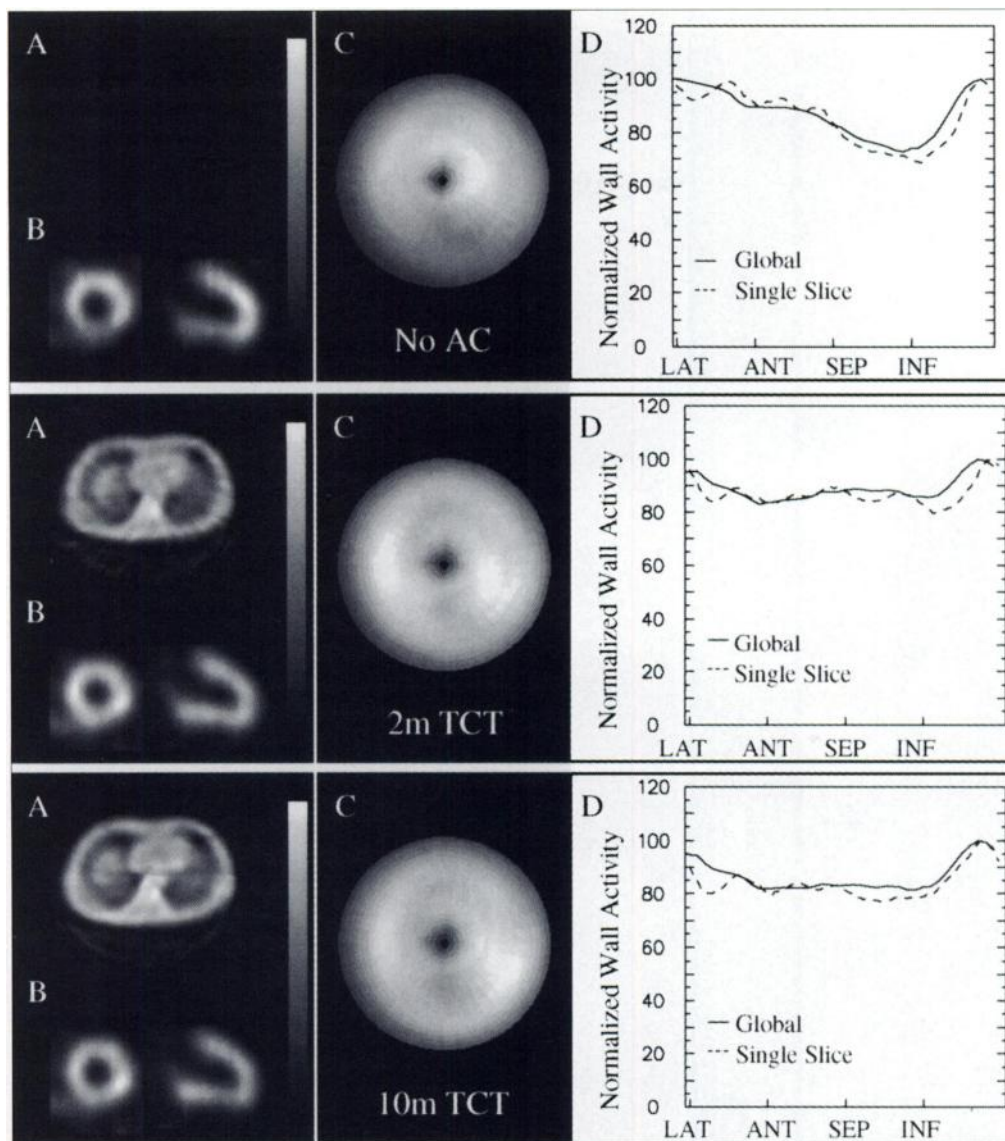


FIGURE 5. Results of NC and AC rest ^{201}Tl SPECT imaging for Patient 1. This individual was a 44-yr-old male volunteer without any history of cardiac disease. (A) Single-pixel-thick slice of TCT. (B) Short-axis and vertical long axis slices through region of myocardium that demonstrates most significant attenuation on NC study. (C) Polar map of SPECT data. (D) Summed circumferential profiles for SA slice shown in B and for myocardium as a whole (global profile).

counts in the TCT are from the ^{201}Tl emission source, and the projection with the highest crosstalk has only 0.63% of its counts contributed by ^{201}Tl . This form of crosstalk will, of course, be increased if the emission source energy is equivalent to or higher than the transmission source energy (34). However, because a high-activity line source is used, the crosstalk fraction in the TCT should remain below 5–10% even when the emission energy is higher than the transmission energy. For example, for a crosstalk measurement with a ^{153}Gd TCT source and a $^{99\text{m}}\text{Tc}$ ECT source, on average, $3.4 \pm 1.3\%$ of counts in the AsF-TCT are from $^{99\text{m}}\text{Tc}$. In this study, no crosstalk correction was used because the magnitude of the crosstalk is $<1\%$. However, if a crosstalk correction is desired, an effective correction could be obtained by acquiring emission data in the transmission energy window with the AsF collimator during the ECT acquisition. These AsF-ECT data could be scaled to compensate for the different ECT and TCT acquisition durations and subtracted from the TCT projections to compensate for emission photons present in the TCT.

For both simultaneous and sequential protocols, image quality is degraded if the patient moves during the study. With simultaneous protocols, patient motion will degrade the ECT

and the TCT at the same time. Thus, the motion-correction algorithm would need to be applied to both studies. Patient motion during a sequential protocol could result in a TCT that is not spatially registered with the ECT study. However, for cases where motion is suspected, the TCT can be manually reregistered with the ECT study. Currently, this is done by subjectively translating the attenuation map (TCT) to match the ECT data. However, more sophisticated protocols could be developed to assist in registering the two acquisitions (35). Furthermore, acquiring the ECT and the TCT separately presents the possibility that one acquisition could be repeated independently of the other to compensate for patient motion. In general, however, the best way to address patient motion is to reduce the total imaging time required.

The geometry of the SPECT system also imposes several constraints on the type of AC technique that can be used. For example, implementing scanning line source techniques on a triple-head SPECT system is difficult, while the geometry of L-shaped double-head SPECT systems is quite amenable to such techniques. This consideration is particularly important in developing AC protocols for existing camera systems. Using a simultaneous protocol on a triple-head SPECT system can also

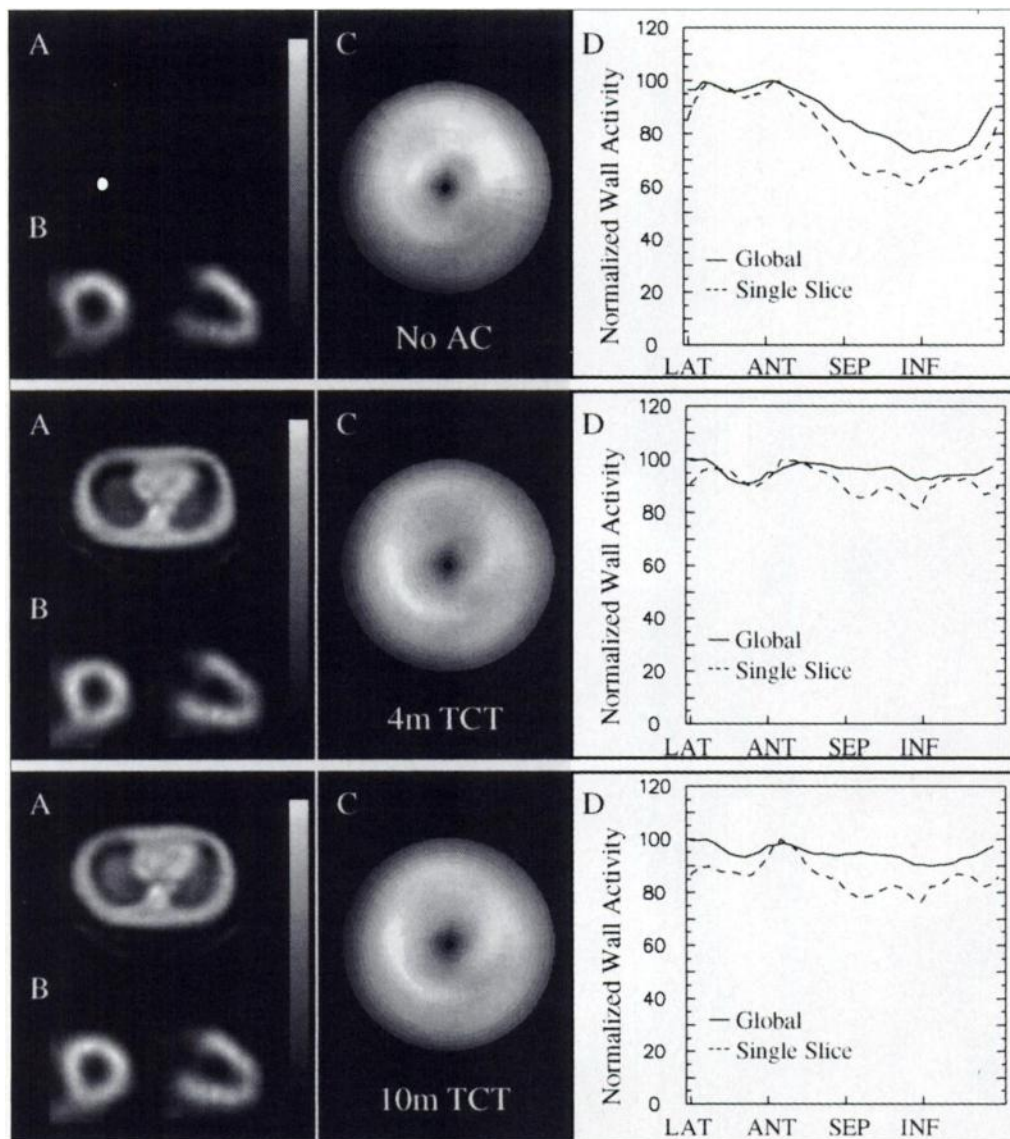


FIGURE 6. Results of NC and AC stress ^{201}Tl SPECT imaging for Patient 2. This individual was a 37-yr-old man who complained of chest pain but had no other clinical evidence of cardiac disease. (A) Single-pixel-thick slice of TCT. (B) Short-axis and vertical long axis slices of portion of myocardium that demonstrates most significant attenuation on NC study. (C) Polar map of SPECT data. (D) Summed circumferential profiles for SA slice shown in B and for myocardium as a whole (global profile).

impose constraints on the ECT acquisition; for example, the radius of rotation of all of the heads may need to be increased so that they do not block the edges of a fanbeam TCT. This limitation would be particularly significant for a simultaneous protocol using AsF collimation on a triple-head system because the radius of rotation of the camera holding the source would need to be large and because the source holder would block a portion of this camera. Therefore, we believe that the best application of the AsF geometry is with a sequential imaging protocol.

In PET, attenuation correction using transmission data that are noisy relative to the emission data has been shown to cause artifacts in the reconstructed images. Smoothing of the transmission scans has been proposed as a way to address this problem (36,37). We have performed preliminary investigations to determine whether augmenting the filtered backprojection reconstruction of the AsF-TCT by smoothing the data allows use of shorter duration TCTs. These results indicate that separately smoothing either the projection data or the reconstructed TCT before ML-EM reconstruction of the AC study does not significantly alter the AC results. This is consistent

with simulation studies that indicated that the noise content of attenuation-corrected SPECT images is dominated by the statistical quality of the ECT rather than that of the TCT (24). However, we are exploring smoothing combined with segmentation of the central portion of the thorax as a way to eliminate the hole artifact encountered with short-duration TCTs.

This study has several limitations. First, no scatter correction was applied. As is evidenced by the phantom images in Figure 3, after AC, some nonuniformities remain. This effect may be emphasized in phantom studies because the same geometry that results in significantly nonuniform attenuation also results in nonuniform scatter conditions. However, most of the scatter correction algorithms under development by others could be used in conjunction with AsF-based AC to compensate for both attenuation and scatter. Using explicit scatter correction with subsequent readjustment of the attenuation coefficients used in the ML reconstruction could further improve the quantitative accuracy of the reconstructed SPECT images.

Second, for this study a refillable $^{99\text{m}}\text{Tc}$ line source was used. The activity of the source was chosen to provide an average transmission CR of ~ 40 kcps. Because of the nonuniform

incident photon flux, this is approximately the maximum CR that can be obtained without introducing count losses for the camera used in this study (38). Using a fillable line source allows the source activity and length to be changed easily. Although this is beneficial during pilot studies of the technique, routine use of a refillable source is not desirable because of the radiation exposure received during filling. Several groups have investigated longer half-life sources for transmission imaging (39–41). We are currently modifying the AsF protocol to make use of a ^{153}Gd source and a tin wedge filter. This isotope is available with high activity at a reasonable cost and has a photon energy (100 keV) that is suitable for AC for both ^{201}Tl and $^{99\text{m}}\text{Tc}$ radiopharmaceuticals.

Additionally, the protocol used for this study required that the AsF collimator and source assembly be mounted after the ECT acquisition had been completed. We chose this technique to prevent altering our existing ECT acquisition protocol because the NC studies were used clinically. However, changing collimators is not practical for routine clinical use. One way to address this problem is to acquire the ECT with only the two remaining cameras of the SPECT system. This is consistent with several existing cardiac SPECT protocols that use only two heads of a triple-head SPECT system because the sensitivity of the third camera in a 120° rotation is low. With such a protocol, the source can be quickly mounted (<30 sec) between the ECT and TCT acquisitions. It may also be possible to use the AsF collimator to acquire ECT data. Although this would improve the sensitivity of the system relative to that of a protocol using only two of the three cameras to acquire ECT data, AsF emission data from the heart are missing or truncated in some projection views. This requires modifying the ECT reconstruction algorithm. Further studies are needed to determine the optimal way to combine AsF and parallel (or other cardiac-specific geometry) ECT data to increase the system sensitivity during the emission study.

We are also continuing to investigate ways to modify the AsF geometry to further increase the transmission FOV. Recently, results of a simulation study using a longer focal length AsF to obtain a somewhat larger FOV were presented (33). This method appears promising; however, the design of some triple-head gamma cameras (such as the one used in this study) with the cameras mounted inside the gantry precludes extending the focal length of the fanbeam significantly beyond the current 52 cm.

CONCLUSION

A triple-head SPECT system fitted with a $^{99\text{m}}\text{Tc}$ line source and AsF collimator was used to demonstrate that attenuation maps from short-duration, sequential TCT imaging can be used to improve the uniformity of SPECT measurements of myocardial tracer uptake. A 4-min TCT provides an attenuation map that is suitable for correcting ECTs acquired with a conventional clinical protocol. With a high CR SPECT system, it should be possible to further reduce the duration of the TCT. The entire AC imaging protocol can be performed in just over 20 min.

Using short-duration, sequential TCT for AC has several advantages. First, acquisition of the TCT does not alter the acquisition of the ECT, and it eliminates the effects of crosstalk in the emission study. Second, using a high-activity line source reduces the effects of emission source crosstalk on the TCT and allows a short-duration TCT acquisition. Finally, a sequential TCT acquisition does not limit the types of ECT protocols that can be used, e.g., by requiring a 360° camera rotation or increasing the camera radius of rotation. Short-duration, se-

quential AsF-TCT shows promise as a means for implementing AC in cardiac SPECT imaging. Although the results of clinical AC studies have, to date, shown great promise, additional studies with large patient populations are needed to further demonstrate the diagnostic value of AC for cardiac SPECT.

ACKNOWLEDGMENTS

We are grateful for the assistance of Drs. Ernest Fordham and Clark Nolan during the clinical aspects of this study. Many helpful discussions with Drs. Donald Gunter, Jingai Liu, Kenneth Matthews and Caesar Ordonez are also appreciated. We thank Nuclear Fields for the loan of the AsF collimator. This work was supported in part by National Cancer Institute Grant CA51329 and by a Rush University Office of Research Administration Institutional Grant.

REFERENCES

- Li J, Jaszczak RJ, Greer KL, Gilland DR, DeLong DM, Coleman RE. Evaluation of SPECT quantification of radiopharmaceutical distribution in canine myocardium. *J Nucl Med* 1995;36:278–286.
- LaCroix DJ, Tsui BMW. The effect of defect size, location and contrast on the diagnosis of myocardial defects in SPECT images with and without attenuation correction [Abstract]. *J Nucl Med* 1996;37:210P.
- DiBella EVR, Eisner RL, Schmarkey LS, et al. Heterogeneity of SPECT bull's-eyes in normal dogs: comparison of attenuation compensation algorithms. *IEEE Trans Nucl Sci* 1995;42:1290–1296.
- Ficaro EP, Fessler JA, Shreve PD, Kritzman JN, Rose PA, Corbett JR. Simultaneous transmission/emission myocardial perfusion tomography. *Circulation* 1996;93:463–473.
- Chang LT. A method for attenuation correction in radionuclide CT. *IEEE Trans Nucl Sci* 1978;25:638–643.
- Bateman TM, Kolobrodov VV, Vasin AP, O'Keefe JH. Extended acquisition for minimizing attenuation artifact in SPECT cardiac perfusion imaging. *J Nucl Med* 1994;35:625–627.
- Segall GM, Davis MJ. Prone versus supine thallium myocardial SPECT: a method to decrease artifactual inferior wall defects. *J Nucl Med* 1989;30:548–555.
- Frey EC, Tsui BMW, Perry JR. Simultaneous acquisition of emission and transmission data for improved thallium-201 cardiac SPECT imaging using a technetium-99m transmission source. *J Nucl Med* 1992;33:2238–2245.
- Tung C-H, Gullberg GT, Zeng GL, Christian PE, Datz FL, Morgan HT. Non-uniform attenuation correction using simultaneous transmission and emission converging tomography. *IEEE Trans Nucl Sci* 1992;39:1134–1143.
- Tan P, Bailey DL, Meikle SR, Eberl S, Fulton RR, Hutton BF. A scanning line source for simultaneous emission and transmission measurements in SPECT. *J Nucl Med* 1993;34:1752–1760.
- Larsson SA, Kimiaei S, Ribbe T. Simultaneous SPECT and CT with shutter controlled radionuclide sources and parallel collimator geometry. *IEEE Trans Nucl Sci* 1993;40:1117–1122.
- Ficaro EP, Fessler JA, Ackermann RJ, Rogers WL, Corbett JR, Schwaiger M. Simultaneous transmission-emission thallium-201 cardiac SPECT. Effect of attenuation correction on myocardial tracer distribution. *J Nucl Med* 1995;36:921–931.
- Malko JA, Van Heertum RL, Gullberg GT, Kowalsky GT. SPECT liver imaging using an iterative attenuation correction algorithm and an external flood source. *J Nucl Med* 1986;27:701–705.
- Tsui BMW, Gullberg GT, Edgerton ER, et al. Correction of nonuniform attenuation in cardiac SPECT imaging. *J Nucl Med* 1989;30:497–507.
- Manglos SH, Bassano DA, Thomas FD, Grossman ZD. Imaging of the human torso using cone-beam transmission CT implemented on a rotating gamma camera. *J Nucl Med* 1992;33:150–156.
- Jaszczak RJ, Gilland DR, Hansen MW, Jang S, Greer KL, Coleman RE. Fast transmission CT for determining attenuation maps using a collimated line source, rotatable air-copper-lead attenuators and fan beam collimation. *J Nucl Med* 1993;34:1577–1586.
- Chang W, Loncaric S, Huang G, Ni B, Liu J. Asymmetrical-fan transmission CT on SPECT to derive μ -maps for attenuation correction [Abstract]. *J Nucl Med* 1994;35:92P.
- Hawman EG, Ficaro EP, Hamill JJ, Schwaiger M. Fanbeam collimation with off-center focus for simultaneous emission/transmission SPECT in multi-camera SPECT systems [Abstract]. *J Nucl Med* 1994;35:92P.
- Chang W, Loncaric S, Huang G, Sanpitak P. Asymmetric fan transmission CT on SPECT systems. *Phys Med Biol* 1995;40:913–928.
- Jaszczak RJ, Gilland DR, McCormick JW. The effect of truncation reduction in fan beam transmission for attenuation correction of cardiac SPECT. *IEEE Trans Nucl Sci* 1996;43:2255–2262.
- Loncaric SL, Chang W, Huang G. Using simultaneous transmission and scatter SPECT imaging from external sources for the determination of the thoracic μ -map. *IEEE Trans Nucl Sci* 1994;41:1601–1606.
- Pan TS, King MA, Penney BC, Rajeevan N, Luo D-S, Case JA. Reduction of truncation artifacts in fan beam transmission by using parallel beam emission data. *IEEE Trans Nucl Sci* 1995;42:1310–1320.
- Madsen MT, Kirchner PT, Edlin J, Nathan M, Kahn D. Emission based technique for obtaining attenuation correction data in myocardial SPECT studies. *Nucl Med Commun* 1993;14:689–695.
- Tung C-H, Gullberg GT. A simulation of emission and transmission noise propagation

- in cardiac SPECT imaging with nonuniform attenuation correction. *Med Phys* 1994;21:1565-1576.
25. Loncaric S, Chang W, Huang G, Hollinger EF. Analysis of the noise characteristics of the attenuation maps obtained with the asymmetric-fan (AsF) sampling on SPECT systems [Abstract]. *J Nucl Med* 1995;36:169P.
 26. Kemp BJ, Prato FS, Nicholson RL, Reese L. Transmission CT imaging of the head with a SPECT system and a collimated line source. *J Nucl Med* 1995;36:328-335.
 27. Loncaric S, Chang W, Huang G. A processing technique for the truncated projections of asymmetric-fanbeam transmission imaging. *IEEE Trans Nucl Sci* 1995;42:2292-2297.
 28. Attix FH. *Introduction to radiological physics and radiation dosimetry*. New York: Wiley; 1986:556-561.
 29. Shepp LA, Vardi Y. Maximum likelihood reconstruction for positron emission tomography. *IEEE Trans Med Imag* 1982;1:113-121.
 30. Garcia EV, Van Train K, Maddahi J, et al. Quantification of rotational thallium-201 myocardial tomography. *J Nucl Med* 1985;26:17-26.
 31. Tsui BMW, Zhao XD, Gregoriou GK, et al. Quantitative cardiac SPECT reconstruction with reduced image degradation due to patient anatomy. *IEEE Trans Nucl Sci* 1994;41:2838-2844.
 32. Li J, Tsui BMW, Welch A, Frey EC, Gullberg GT. Energy window optimization in simultaneous technetium-99m TCT and thallium-201 SPECT data acquisition. *IEEE Trans Nucl Sci* 1995;42:1207-1213.
 33. Gilland DR, Wang H, Coleman RE, Jaszczak RJ. Long focal length, asymmetric fan beam collimation for transmission acquisition with a triple camera SPECT system. *IEEE Trans Nucl Sci* 1997;44:1191-1196.
 34. Kiat H, Germano G, Friedman J, et al. Comparative feasibility of separate or simultaneous rest thallium-201/stress technetium-99m-sestamibi dual-isotope myocardial perfusion SPECT. *J Nucl Med* 1994;35:542-548.
 35. Levin DN, Pelizzari CA, Chen CT, Chen GT, Cooper MD. Retrospective geometric correlation of MR, CT, and PET images. *Radiology* 1988;169:817-823.
 36. Meikle SR, Dahlbom M, Cherry SR. Attenuation correction using count-limited transmission data in positron emission tomography. *J Nucl Med* 1993;34:143-150.
 37. Freedman NMT, Bacharach SL, Carson RE, Price JC, Dilsizian V. Effect of smoothing during transmission processing on quantitative cardiac PET scans. *J Nucl Med* 1996;37:690-694.
 38. Huang G, Ni B, Chang W, Loncaric S. High count-rate transmission CT on a SPECT system [Abstract]. *J Nucl Med* 1994;35:192P.
 39. Ficaro EP, Fessler JA, Rogers WL, Schwaiger M. Comparison of americium-241 and technetium-99m as transmission sources for attenuation correction of thallium-201 SPECT imaging of the heart. *J Nucl Med* 1994;35:652-663.
 40. Frey EC, Tsui BMW. A comparison of Gd-153 and Co-57 as transmission sources for simultaneous TCT and Tl-201 SPECT. *IEEE Trans Nucl Sci* 1995;42:1201-1206.
 41. Wang H, Jaszczak RJ, McCormick JW, Greer KL, Coleman RE. Experimental evaluation of tellurium-123m transmission source to determine attenuation maps for SPECT. *IEEE Trans Nucl Sci* 1995;42:1214-1219.

EDITORIAL

Innovative Design Concepts for Transmission CT in Attenuation-Corrected SPECT Imaging

Photon attenuation in cardiac SPECT is the major factor that contributes to quantitative inaccuracies when measuring in vivo distribution of radioactivity. The application of nonuniform attenuation correction significantly improves image uniformity of myocardial tracer distribution. In the article by Hollinger et al. (1), a compelling advancement in the technologic development of attenuation correction in SPECT imaging is presented. Hollinger et al. investigated the feasibility of using an asymmetric fanbeam geometry with a radioactive line source to acquire transmission CT (TCT) on a triple-head SPECT system to correct for photon attenuation in cardiac SPECT. What makes their work significant is that it provides a solution to the truncation problem that has slowed the acceptance of TCT with three-detector SPECT systems when simultaneously implemented with emission imaging (2).

The asymmetric fanbeam provides a means for obtaining truncation-free transmission images with a fixed line source not only for three-detector SPECT systems but also one- and two-detector SPECT systems. When only a portion of the field of view for a particular angular projection is covered, an individual projection can be completed by using the proper conjugate views from a 360° acquisition. The integration of TCT into

SPECT systems has posed some challenges that have been the impetus for various innovative design concepts of which asymmetric fanbeam geometry is an important example. These developments also have led researchers to consider incorporating asymmetric cone-beam geometries in the design of future SPECT systems.

A variety of TCT design concepts have been proposed for commercial SPECT systems. The designers of these systems have struggled with numerous decisions, including whether to use sequential (3-6) or simultaneous transmission and emission (7-11) imaging; whether to use parallel (3-7), fanbeam (6,8,11,12), asymmetric fanbeam (1,13) or cone-beam (14) collimation; whether to use single-detector (3-5) or multiple-detector (6,8) systems; whether to use flood (3,5), scanning line (7,10), fixed point (14), single fixed line (6,7,11,12) or multiple fixed line (15) sources; and whether to use an x-ray tube (16) or gamma ray transmission sources (1-15).

In early work, the TCT study was performed before the emission study using a flood source mounted opposite a single, parallel-collimated detector (3,5). Unfortunately, this arrangement increased patient scan time, increased bulk and weight that was a result of the plane source and derived poor transmission statistics because of parallel collimation. Improvements were made by placing the transmission

source at the focus of a converging collimator, such as a cone-beam or fanbeam collimator. However, the disadvantage of converging collimation is the truncation of transmission data that occurs with typical wide-field-of-view gamma cameras. A scanning line source with a parallel collimator reduces the truncation problem experienced with converging collimation (10). By electronically blanking the detector and zeroing in on the transmission energy, these systems can reconstruct distributions of narrow beam attenuation coefficients. However, the implementation by a motor-driven scanning line source and electronic blanking of camera electronics can be more complicated and more expensive than using a fixed line source. Parallel collimation also lowers the geometric efficiency and thereby requires increased source strengths that result in higher scatter-to-primary ratios and higher patient doses than occur with a line source placed at the focal line of a fanbeam collimator or a point source placed at the focal point of a cone-beam collimator.

Therefore, it is of particular interest to manufacturers to use a fixed source rather than a moving source. If a single, fixed, line source is used, then some type of fanbeam collimation is required. Using asymmetric or half fanbeam geometry, the truncation problem can be eliminated by assimilating projection samples over 360°. This means that a dual-detector system mounted with half fanbeam collimators placed orthogonal to each other can eliminate the truncation problem if each camera is rotated 180°.

Another article to appear in an upcoming issue of *The Journal of Nuclear Medicine*

Received Apr. 17, 1998; accepted Apr. 28, 1998.

For correspondence or reprints contact: Grant T. Gullberg, PhD, Medical Imaging Research Laboratory, Department of Radiology, University of Utah, 729 Arapahoe Dr., Salt Lake City, UT 84108-1218.